



TM4SF19 controls GABP-dependent YAP transcription in head and neck cancer under oxidative stress conditions

Eunbie Shin^a, Yongsoo Kwon^a , Eunji Jung^a , Yong Joon Kim^b , Changgon Kim^a, Semyeong Hong^a, and Joon Kim^{a,1}

Edited by Moshe Oren, Weizmann Institute of Science, Rehovot, Israel; received August 29, 2023; accepted January 4, 2024

Tobacco and alcohol are risk factors for human papillomavirus-negative head and neck squamous cell carcinoma (HPV⁻ HNSCC), which arises from the mucosal epithelium of the upper aerodigestive tract. Notably, despite the mutagenic potential of smoking, HPV⁻ HNSCC exhibits a low mutational load directly attributed to smoking, which implies an undefined role of smoking in HPV⁻ HNSCC. Elevated *YAP* (Yes-associated protein) mRNA is prevalent in HPV⁻ HNSCC, irrespective of the *YAP* gene amplification status, and the mechanism behind this upregulation remains elusive. Here, we report that oxidative stress, induced by major risk factors for HPV⁻ HNSCC such as tobacco and alcohol, promotes *YAP* transcription via TM4SF19 (transmembrane 4 L six family member 19). TM4SF19 modulates *YAP* transcription by interacting with the GABP (Guanine and adenine-binding protein) transcription factor complex. Mechanistically, oxidative stress induces TM4SF19 dimerization and topology inversion in the endoplasmic reticulum membrane, which in turn protects the GABP β 1 subunit from proteasomal degradation. Conversely, depletion of TM4SF19 impairs the survival, proliferation, and migration of HPV⁻ HNSCC cells, highlighting the potential therapeutic relevance of targeting TM4SF19. Our findings reveal the roles of the key risk factors of HPV⁻ HNSCC in tumor development via oxidative stress, offering implications for upcoming therapeutic approaches in HPV⁻ HNSCC.

oral squamous cell carcinoma | L6 tetraspanin | oxidative stress | YAP

Head and neck squamous cell carcinoma (HNSCC) originates from the mucosal epithelium of the anatomical structures constituting the upper aerodigestive tract. It is the sixth most widespread cancer globally and has a mortality rate of 40 to 50% (1). Recently, there has been a marked increase in the incidence of oropharyngeal tumors resulting from human papillomavirus (HPV) infection (2–4). Patients with HPV-positive (HPV⁺) oropharyngeal cancer generally exhibit a more favorable prognosis compared to those with HPV-negative (HPV⁻) oropharyngeal cancer (5). The primary risk factors for HPV⁻ HNSCC include tobacco consumption and alcohol abuse (6). Additionally, areca nut chewing is associated with oral cavity cancer in some Asia-Pacific populations (6). Tobacco, alcohol, and areca nuts produce metabolic by-products that, upon absorption, bind to DNA and cause DNA damage (6). Intriguingly, a recent analysis of the cancer genome indicated that smoking does not significantly increase the mutational load in oral cancer (7), suggesting mechanisms other than direct DNA damage may be contributing to the promotion of HPV⁻ HNSCC development induced by smoking.

Reactive oxygen species (ROS) production is commonly increased in cancer cells due to factors such as high metabolic rate, hypoxia, and gene mutations that affect cell proliferation and mitochondrial function (8). To counterbalance the elevated ROS levels, the nuclear factor erythroid-2-related factor 2 (NRF2) up-regulates the expression of antioxidant pathway genes (9). In the presence of environmental factors that further augment ROS levels in cancer cells, the antioxidant system becomes overloaded, leading to transient oxidative damage. Both the gas and tar phases of tobacco contain substantial amounts of free radicals (10, 11), and alcohol exposure independently increases ROS production via oral acetaldehyde formation, irrespective of hepatic metabolism (10, 11). Oxidative stress can foster cancer development through the activation of oncogenic pathways, disturbance of proteostasis, and induction of DNA damage (12). Conversely, high levels of ROS can trigger various ROS-induced cell death pathways (13). The specific mechanisms by which cancer cells avoid death under conditions of transiently high oxidative stress, such as those encountered during simultaneous tobacco and alcohol consumption, remain elusive.

The transcriptional regulator Yes-associated protein (YAP) is a crucial effector of the Hippo-YAP signaling pathway, dysregulation of which has been observed in a broad range of human cancers (14). Moreover, YAP activity is positively correlated with poor prognostic outcomes and therapeutic resistance in several types of cancers, including HNSCC (15).

Significance

While tobacco and alcohol are risk factors for HPV-negative head and neck squamous cell carcinoma (HPV⁻ HNSCC), their oncogenic role related to oxidative stress is unclear. Additionally, the underlying mechanism for the elevated expression of *YAP*, a critical oncogenic factor, in HPV⁻ HNSCC remains elusive. Here, we report TM4SF19 (transmembrane 4 L six family member 19) as an oxidative stress-dependent activator of *YAP* transcription. TM4SF19 dimerization under oxidative stress upregulates *YAP* expression, clarifying the impact of smoking and alcohol in HPV⁻ HNSCC. Notably, suppressing TM4SF19 significantly reduces oncogenic activity of HPV⁻ HNSCC cells. Our findings reveal the mechanism of how oxidative stress from smoking and drinking facilitates HPV⁻ HNSCC progression, offering a potential therapeutic target for HPV⁻ HNSCC.

Author affiliations: ^aGraduate School of Medical Science and Engineering, Korea Advanced Institute of Science and Technology, Daejeon 34141, Korea; and ^bDepartment of Ophthalmology, Severance Hospital, Institute of Vision Research, Yonsei University College of Medicine, Seoul 03722, South Korea

Author contributions: E.S., E.J., and J.K. designed research; E.S., Y.K., C.K., and S.H. performed research; E.S. and Y.J.K. analyzed data; and E.S. and J.K. wrote the paper.

The authors declare no competing interest.

This article is a PNAS Direct Submission.

Copyright © 2024 the Author(s). Published by PNAS. This article is distributed under Creative Commons Attribution-NonCommercial-NoDerivatives License 4.0 (CC BY-NC-ND).

¹To whom correspondence may be addressed. Email: joonkim@kaist.ac.kr.

This article contains supporting information online at <https://www.pnas.org/lookup/suppl/doi:10.1073/pnas.2314346121/-DCSupplemental>.

Published February 5, 2024.

In the canonical Hippo pathway, a kinase cascade consisting of the mammalian sterile 20-like kinase 1/2 and the large tumor suppressor 1/2 (LATS1/2) acts to negatively regulate the activities of YAP and its paralog the transcriptional coactivator with PDZ-binding motif (TAZ) (16). Upon inactivation of the Hippo kinases, YAP and TAZ enter the nucleus and stimulate transcription of prosurvival genes (17, 18). Genes encoding Hippo kinases and their adapters are mutated or deleted at high rates in mesothelioma and kidney renal papillary cell carcinoma (14). In HNSCC, 50% exhibit somatic alterations in the Hippo-YAP pathway, with 29% showing FAT atypical cadherin 1 (FAT1) mutations resulting in YAP activation (19). Additionally, the actin like 6A (ACTL6A) and p63 collaborate as oncogenic drivers in HNSCC, promoting proliferation and suppressing differentiation through YAP activation, with correlated expression patterns predicting poor patient survival (20). Frequent amplification of *YAP1* and *TAZ* genes specifically occurs in squamous cell-derived cancers, such as HNSCC and cervical squamous cell carcinoma (CESC) (14). This frequent gene amplification suggests that elevated levels of *YAP/TAZ* expression play a pivotal role in the development of HNSCC and CESC.

While a variety of mechanisms regulating YAP protein activity within the context of Hippo signaling are known, our understanding of the transcriptional regulation of YAP remains limited. It has been established that c-Jun, β -catenin, and microRNA-375 are involved in the regulation of *YAP1* mRNA levels (21–24). Recently, it was discovered that the ETS (E26-associated virus transformation-specific) transcription factor GA-binding protein (GABP) binds to the *YAP1* promoter and induces *YAP1* gene transcription in liver cancer (25). Members of the ETS family play a crucial role in regulating cell proliferation, differentiation, and the development of tissues. (26). These proteins are controlled by complex inter- and intramolecular interactions, and their altered expression or activity is frequently observed in cancer. The GABP complex consists of GABP α and GABP β subunits, with GABP α responsible for binding to the promoter region and GABP β contributing to complex formation (27). GABP proteins are widely expressed and control the expression of genes required for various biological processes, including mitochondrial biogenesis, cell proliferation, and immunity (27). Additionally, GABP selectively activates mutant telomerase reverse transcriptase (*TERT*) promoters in human cancers (28). The activity of the GABP complex can be modulated by both the cellular redox state and MAP kinases (29, 30). Oxidation of the cysteine residues of GABP α hampers the interaction between GABP α and GABP β subunits, thereby suppressing their transcriptional activation function in liver cancer (31). It has been suggested that Hippo signaling promotes the inactivation of GABP (25). However, the impact of oxidative stress on GABP-dependent *YAP1* transcription in HNSCC remains unknown.

In this study, we propose a mechanism by which transmembrane 4 L six family member 19 (TM4SF19) enhances *YAP1* gene transcription in HPV $^-$ HNSCC under conditions of oxidative stress. TM4SF19 is a member of the transmembrane 4 L six family (L6 family), which shares topological similarities with genuine tetraspanins (32). Tetraspanin family members contain four transmembrane domains, short N-terminal and C-terminal cytoplasmic tails, short extracellular and intracellular loops, and a longer second extracellular loop near the C terminus (32, 33). The longer extracellular loop encompasses most known binding sites for tetraspanin-interacting proteins, such as integrins and receptor tyrosine kinases (33). TM4SF1 has been implicated in the regulation of cell growth, metastasis, and angiogenesis in cancer (34–37). TM4SF5 has been identified as a therapeutic target for

hepatocellular carcinoma (38). The upregulation of TM4SF19 is associated with afatinib resistance in lung cancer (39) and radiation resistance in prostate cancer (40). However, the biological functions and action mechanisms of TM4SF19 are poorly understood.

Here, we present evidence that TM4SF19 transiently upregulates *YAP1* gene expression in response to oxidative stress in HPV $^-$ HNSCC cells. We found that TM4SF19 enhances *YAP1* transcription by preventing proteasomal degradation of GABP β 1. TM4SF19 depletion reduces GABP β 1 levels, leading to *YAP1* expression downregulation in HPV $^-$ HNSCC cells. We observed that oxidative stress activates TM4SF19 through its dimerization and topology inversion in the endoplasmic reticulum (ER) membrane. Furthermore, TM4SF19 knockdown significantly decreases survival, proliferation, and migration of HPV $^-$ HNSCC cells. Our findings provide insights into the mechanisms by which smoking and alcohol consumption contribute to the development and progression of HPV $^-$ HNSCC.

Results

Oxidative Stress Up-Regulates GABP-Dependent *YAP* Transcription in HPV $^-$ HNSCC Cells. According to The Cancer Genome Atlas (TCGA) data, the *YAP1* gene is amplified at high frequencies in HPV $^-$ HNSCC and CESC (41). In line with this, a subset of HPV $^-$ HNSCC and CESC tissues express *YAP1* mRNA at substantially higher than average levels (SI Appendix, Fig. S1A). Even when considering only cancer samples without apparent *YAP1* gene amplification, HPV $^-$ HNSCC exhibited the highest average *YAP1* mRNA level (Fig. 1A). This suggests that elevated *YAP1* mRNA expression in HPV $^-$ HNSCC is not solely due to gene amplification. The expression of YAP/TEAD direct target genes is also significantly elevated in tumor samples from HPV $^-$ HNSCC patients compared to normal samples, indicating YAP activation in HPV $^-$ HNSCC (SI Appendix, Fig. S1B).

To investigate the impact of external stress on *YAP1* gene expression, we exposed OSCC, a prevalent subtype of HPV $^-$ HNSCC, cell lines YD10B and SCC25 to various stressors: heat shock (45 °C), DNA damage (etoposide), oxidative stress (H₂O₂), and ER stress (thapsigargin and tunicamycin). Of these, only oxidative stress significantly elevated *YAP1* mRNA levels in both cell lines (Fig. 1B). Treatment with H₂O₂ increased the expression of *YAP1*, as well as the oxidative stress response gene *HO-1*, within 20 min (Fig. 1C and SI Appendix, Fig. S1C). Furthermore, when benzo[a]pyrene (BaP), the major carcinogen in tobacco smoke, was introduced to the cell culture, the expression of *YAP1* and *HO-1* genes increased over a similar time course (Fig. 1D and SI Appendix, Fig. S1D). A significant correlation between *YAP1* and *HO-1* mRNA levels was also observed in tumor xenografts intratumorally injected with the oxidative stress inducer diethyl maleate (DEM) (Fig. 1E). These results suggest that upregulation of *YAP1* is an early response to oxidative stress in OSCC cells.

We next investigated which transcription factors might be responsible for the upregulation of *YAP1* expression in response to oxidative stress. Utilizing transcription factor binding prediction software (CiiIDER), we identified several potential candidates capable of binding to the promoter region of the *YAP1* gene, including three previously reported transcription factors: CREB, GABP, and TCF4. Of these, our focus was primarily on GABP, given its known regulation by oxidative stress (25). We constructed vectors with a *YAP1* promoter truncation fused with the luciferase gene, varying the number of GABP α binding sites. The construct containing a 570 bp DNA fragment from the *YAP1* promoter (pGL3-Y570) exhibited the highest luciferase activity (SI Appendix,

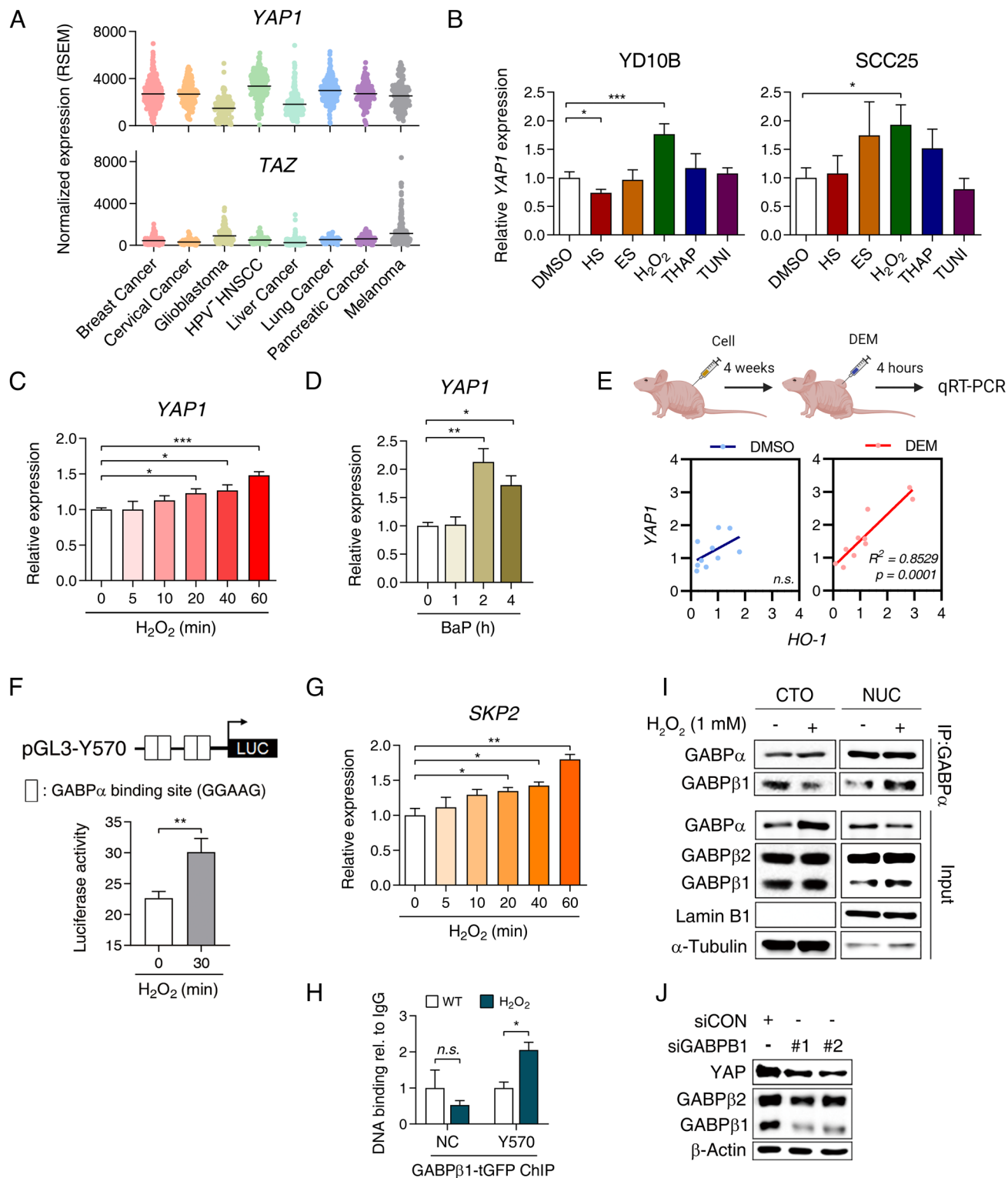


Fig. 1. *YAP1* transcription is up-regulated by oxidative stress in HPV[−] HNSCC. (A) *YAP1* and *TAZ* expression levels in diploid cells of different types of human cancers in the TCGA dataset (breast cancer, $n = 479$; cervical cancer, $n = 140$; glioblastoma, $n = 120$; HPV[−] HNSCC, $n = 204$; liver cancer, $n = 254$; lung cancer, $n = 224$; pancreatic cancer, $n = 143$; melanoma, $n = 163$). (B) qRT-PCR analysis of *YAP1* in the indicated HPV[−] HNSCC cells after exposure to various stimuli (HS: heat shock, ES: etoposide, H₂O₂: hydrogen peroxide, THAP: thapsigargin, TUNI: tunicamycin). (C) qRT-PCR analysis of *YAP1* under various time courses of 1 mM H₂O₂ treatment in YD10B cells. Cycloheximide (50 µg/mL) was introduced for 3 h before treating with H₂O₂. (D) qRT-PCR analysis of *YAP1* in YD10B cells under various time courses of 0.5 mM benzo[a]pyrene (BaP) treatment. (E) Correlation between *YAP1* and *HO-1* expressions in xenograft tumors after injection of DMSO or DEM ($n = 10$ in each group). Schematic diagram made in BioRender (<https://biorender.com/>). (F) Luciferase activity of the pGL3-Y570 promoter after treating with 1 mM H₂O₂ for 30 min compared to control in YD10B cells. (G) qRT-PCR analysis of *SKP2* under various time courses of H₂O₂ treatment. YD10B cells were treated the same as in Fig. 1C. (H) ChIP-qPCR results showing the binding of GABPβ1-turboGFP (GABPβ1-tGFP) to a negative control locus (NC) or the *YAP* promoter region (Y570) following H₂O₂ treatment in YD10B cells. DNA binding is expressed as a fraction of the input and normalized against IgG control. (I) Coimmunoprecipitation analysis of GABPα and GABPβ1 in the cytosol (CTO) and nucleus (NUC). YD10B cells were treated with H₂O₂ for 1 h. (J) Western blot of the indicated proteins in YD10B cells transfected with siRNAs targeting GABPB1 for 48 h. (B–D and F–H) Error bars indicate SEM ($n = 3$ independent experiments; * $P < 0.05$, ** $P < 0.01$, and *** $P < 0.001$, unpaired *t* test).

Fig. S1E). Contrary to the findings of a previous study (25) that oxidative stress inhibits GABP activity in liver cancer, we found that H₂O₂ treatment increased luciferase activity driven by the GABP-binding sequence (pGL3-Y570) in YD10B cells (Fig. 1F). Moreover, the transcription of *SKP2*, a GABP target gene, increased over time following H₂O₂ treatment (Fig. 1G). To confirm GABP binding to the *YAP1* promoter region, we performed chromatin immunoprecipitation analysis. We detected specific binding activity of GABP to the 570 bp upstream region (Fig. 1H). GABP subunits function as heterodimers, either GABP α / β 1 or GABP α / β 2 (27). Coimmunoprecipitation analysis of GABP subunits revealed the enhanced physical interactions between GABP α and GABP β 1 in the nucleus under oxidative stress (Fig. 1I), potentially explaining the increased transcriptional activity of the GABP complex. As expected, knockdown of the *GABP1* resulted in decreased YAP expression in YD10B cells (Fig. 1J). These findings suggest a role for the GABP complex in the upregulation of *YAP1* gene transcription in OSCC under oxidative stress conditions.

Depletion of TM4SF19 Reduces YAP Gene Transcription in HPV⁻ HNSCC Cells. We aimed to uncover the upstream regulators that govern GABP-dependent *YAP1* transcription in the context of recurrent oxidative stress in OSCC. First, we selected genes that fulfill two conditions as candidates (*SI Appendix*, Fig. S2A and Table S1): 1) when depleted, they reduce nuclear YAP protein levels but do not affect the nucleocytoplasmic ratio of YAP, based on our previous siRNA library screening data (43, 44); and 2) they are frequently overexpressed and/or amplified in HPV⁻ HNSCC patient samples (TCGA data). We examined the mRNA level of *YAP1* after knockdown of each candidate. Notably, depletion of TM4SF19 resulted in a significant reduction in *YAP1* mRNA levels (Fig. 2 A and B and *SI Appendix*, Fig. S2B). In contrast, TM4SF19 depletion did not significantly change the mRNA level of *TAZ* (*SI Appendix*, Fig. S2C). Among the candidates, *TM4SF19* was found to be the most overexpressed and amplified in HPV⁻ HNSCC patients compared to various cancers or normal tissues and HPV⁺ HNSCC samples (*SI Appendix*, Fig. S2 D and E). There was no correlation between *TM4SF19* and *PIK3CA*, whose locus is close to *TM4SF19* and is highly amplified in various cancers, including HPV⁻ HNSCC (*SI Appendix*, Fig. S2F), indicating that they are independently overexpressed. Moreover, the expression of *TM4SF19* positively correlates with the cancer stage in HPV⁻ HNSCC patients (*SI Appendix*, Table S2).

Immunoblotting analysis confirmed that TM4SF19 knockdown reduced YAP protein levels in YD10B and SCC25 cells (Fig. 2C). Consistent with this, cells depleted of TM4SF19 showed lower levels of anti-YAP immunofluorescence (Fig. 2D). The downregulation of YAP after TM4SF19 knockdown was also observed in LATS1/2-null RPE1 cells, indicating that TM4SF19 functions independently of the Hippo-YAP pathway (*SI Appendix*, Fig. S3A). The amount of YAP protein phosphorylated at S127 and S397 decreased to a similar extent as the total YAP protein, indicating that the reduction in YAP caused by TM4SF19 knockdown was not a result of LATS activation (*SI Appendix*, Fig. S3B). The level of phospho-TAZ protein did not decrease, aligning with the unchanged total TAZ protein (*SI Appendix*, Fig. S3B). As expected, the depletion of TM4SF19 did not affect the nuclear localization of YAP (Fig. 2E). The downregulation of YAP expression was rescued by transfecting cells with an expression vector carrying an siRNA-insensitive form of the *TM4SF19* gene (*SI Appendix*, Fig. S3C). To test whether TM4SF19 influences YAP protein stability in addition to *YAP1* transcription, cells were treated with the proteasomal degradation inhibitor MG132 or the lysosomal degradation

inhibitor bafilomycin A after TM4SF19 knockdown. Neither treatment rescued the decrease in YAP caused by TM4SF19 knockdown (Fig. 2F and *SI Appendix*, Fig. S3D).

After TM4SF19 depletion, approximately 50% of *YAP1* mRNAs remained, and the reduction in nuclear YAP immunofluorescence intensity was even smaller. Next, we examined whether this level of YAP reduction has a significant impact on cell physiology. We identified a concentration of YAP siRNA that reduced *YAP1* mRNA by about 50% and observed a significant decrease in the expression of *YAP1* target genes under this condition (*SI Appendix*, Fig. S3E). Additionally, we noted that the number of Ki-67-positive (Ki-67⁺) cells and cell survival significantly decreased in response to ~50% *YAP1* mRNA reduction (*SI Appendix*, Fig. S3 F and G). However, even when *YAP1* expression was inhibited by ~75% with a higher concentration (20 nM) of siRNA, nuclear fluorescence intensity decreased at a smaller rate, similar to that in TM4SF19 knockdown conditions (*SI Appendix*, Fig. S3 H and I). These results suggest that TM4SF19 knockdown is as effective as the direct suppression of *YAP1* expression. Consistently, the depletion of TM4SF19 also led to the downregulation of the YAP target genes *CTGF* and *CYR61* (Fig. 2G). RNA-seq analysis further demonstrated reduced levels of YAP target gene expression in TM4SF19-depleted YD10B cells (Fig. 2H). Additionally, the activity of a luciferase reporter controlled by the TEAD-binding sequence significantly decreased after TM4SF19 knockdown (*SI Appendix*, Fig. S3J). Collectively, these results suggest that TM4SF19 supports YAP function in OSCC cells by promoting YAP expression at the transcription level.

TM4SF19 Affects YAP Transcription through GABP β 1. To test whether TM4SF19 interacts with GABP to control *YAP1* transcription, we first examined its influence on the expression of *SKP2*. Depletion of TM4SF19 led to a reduction in *SKP2* mRNA levels, while the target genes of other transcription factors known to regulate *YAP1* were not down-regulated by TM4SF19 knockdown (Fig. 3A and *SI Appendix*, Fig. S4 A and B). The expression of pre-miR375, known to inhibit *YAP1* expression, was also unaffected by TM4SF19 knockdown (*SI Appendix*, Fig. S4B) (24). The expression of the *TM4SF19* gene in HPV⁻ HNSCC patients showed positive correlations with *SKP2* and *GABP1*, which encodes an isoform of the GABP β subunit (*SI Appendix*, Fig. S4C). The protein-level coexpression of TM4SF19 and GABP β 1 in HPV⁻ HNSCC cell lines was confirmed by immunoblotting (*SI Appendix*, Fig. S4D). SCC25 cells expressed lower levels of TM4SF19 both in mRNA and protein levels, and *TM4SF19* expression was not detectable in a human fibroblast cell line, GM07522 (*SI Appendix*, Fig. S4E). Next, we investigated whether TM4SF19 affects the expression or activity of the GABP complex in YD10B, SCC25, and LATS1/2-null RPE1 cells. Importantly, depletion of TM4SF19 resulted in a reduction in the protein level of GABP β 1, while other subunits remained unaffected (Fig. 3B and *SI Appendix*, Fig. S4 F and G). Furthermore, inhibition of TM4SF19 expression decreased the luciferase activity driven by the GABP-binding sequence of the *YAP1* promoter (Fig. 3C). The major phosphorylation sites for GABP β are known to be serine 170 (S170) and threonine 180 (T180) (25). Despite the fact that the activity of several Ets transcription factors is typically enhanced by phosphorylation, a previous study demonstrated that phosphorylation of GABP β at S170 suppresses the transcriptional activity of the GABP complex (25). YAP downregulation resulting from TM4SF19 knockdown was partially rescued by wild-type GABP β 1 overexpression (Fig. 3D). Moreover, GABP β 1 with a phospho-blocking mutation at S170 (S170A) also effectively rescued YAP expression, whereas the same mutation at T180

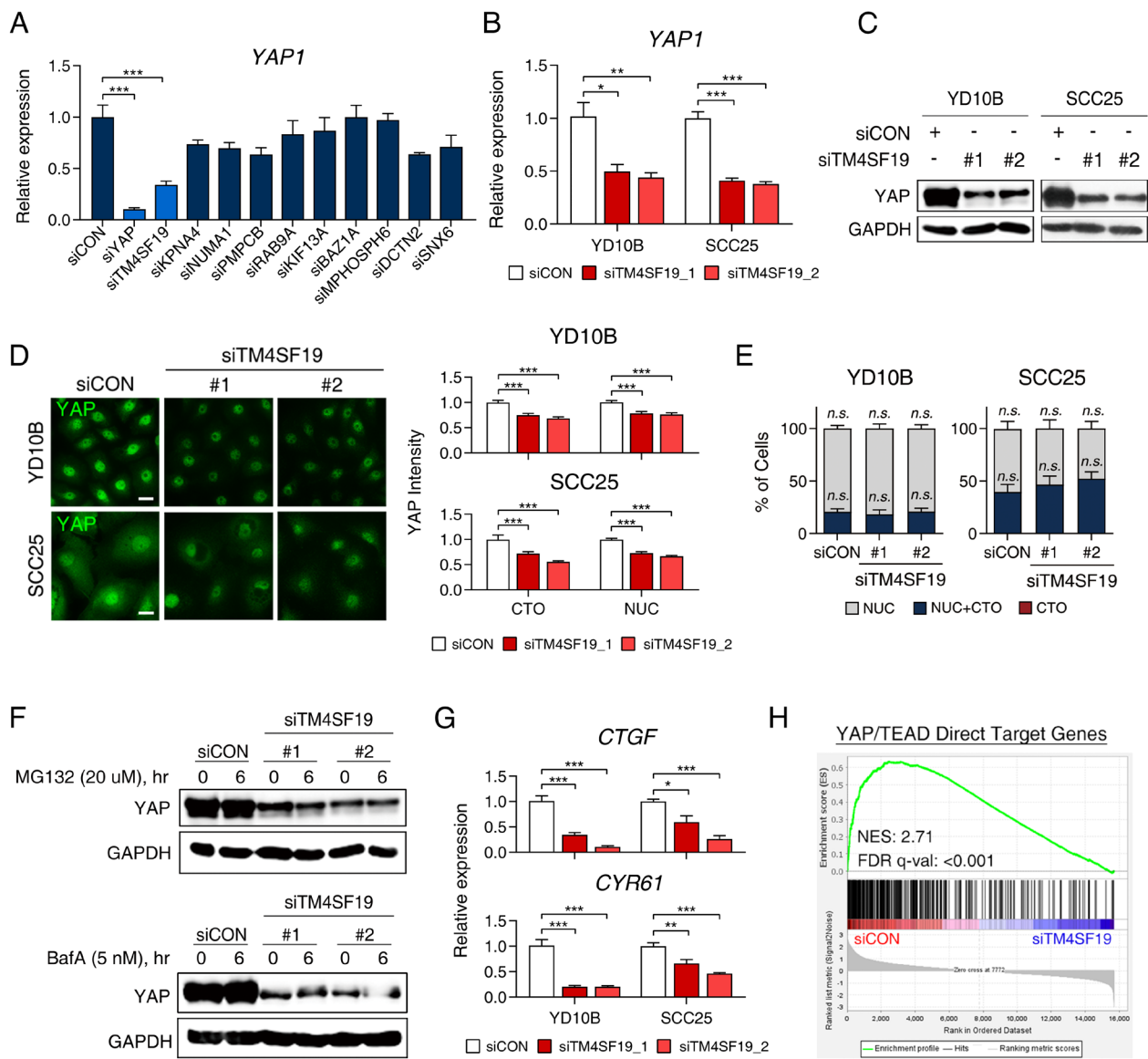


Fig. 2. Depletion of TM4SF19 down-regulates YAP1 transcription in HPV⁻ HNSCC. (A) qRT-PCR analysis of YAP1 in YD10B cells after transfection with a pool siRNAs targeting each candidate of YAP regulator for 48 h. (B) qRT-PCR analysis of YAP1 in YD10B and SCC25 cells after transfection with two distinct siRNAs targeting TM4SF19 for 48 h. (C) Western blot of the indicated proteins in YD10B and SCC25 cells after transfection with siRNAs targeting TM4SF19 for 72 h. (D) Immunofluorescence staining of YAP after transfecting siRNAs targeting TM4SF19 for 72 h (Left, the scale bar represents 15 μ m), and the quantification graphs of its intensity in the cytoplasmic (42) and nuclear (NUC) regions (45). (E) Classification of YAP localization from immunofluorescence images analyzed in Fig. 2D (NUC: nuclear localization, NUC+CTO: nuclear and cytoplasmic localization, CTO: cytoplasmic localization). (F) Western blot of the indicated proteins in YD10B cells. Cells were transfected with siRNAs targeting TM4SF19 for 48 h, followed by the drug treatments as stated. (G) qRT-PCR analysis of CTGF and CYR61 in YD10B and SCC25 cells after transfection with siRNAs targeting TM4SF19 for 48 h. (H) GSEA data of YAP/TEAD direct target gene expressions in TM4SF19 knockdown YD10B cells compared to those with control. Cells were transfected with siRNAs for 48 h. (A, B, D, E, and G) Error bars indicate SEM ($n = 3$ independent experiments; * $P < 0.05$, ** $P < 0.01$, and *** $P < 0.001$, unpaired t test).

(T180A) failed to rescue YAP downregulation (Fig. 3D). The decrease in GABP β 1 expression was partially rescued by treating cells with MG132 after transfection with TM4SF19 siRNAs, whereas baflomycin A treatment had no rescue effect (Fig. 3E). The mRNA levels of GABP subunits were unaffected by TM4SF19 knockdown (SI Appendix, Fig. S4H). Taken together, these results suggest that TM4SF19 is involved in the transcriptional regulation of YAP, at least in part, by blocking proteasomal degradation of GABP β 1.

Oxidative Stress Promotes Cis-Interaction and Topology Inversion of TM4SF19 in the ER Membrane. The L6 family tetraspanins are known to participate in cellular signaling as nanodomains formed through cis-interactions with other family

members and partner proteins (46). We investigated the impact of oxidative stress on potential homomeric cis-interactions of TM4SF19. YD10B cells were transfected with FLAG-tagged TM4SF19 and exposed to various concentrations of H₂O₂ for 10 min. Under nonreducing conditions, TM4SF19 proteins shifted from monomers to dimers in response to H₂O₂ treatment (Fig. 4A). We next examined the oxidation status of TM4SF19 at different time points after H₂O₂ treatment. TM4SF19 dimerization was observed after a 5-min exposure to H₂O₂, while YAP upregulation became apparent after 20 min (Fig. 4B). To validate that the H₂O₂-induced increase in YAP was due to TM4SF19 activation, we depleted TM4SF19 and then treated the cells with H₂O₂. Under TM4SF19 knockdown conditions, H₂O₂ treatment did not lead to an increase in YAP (Fig. 4C).

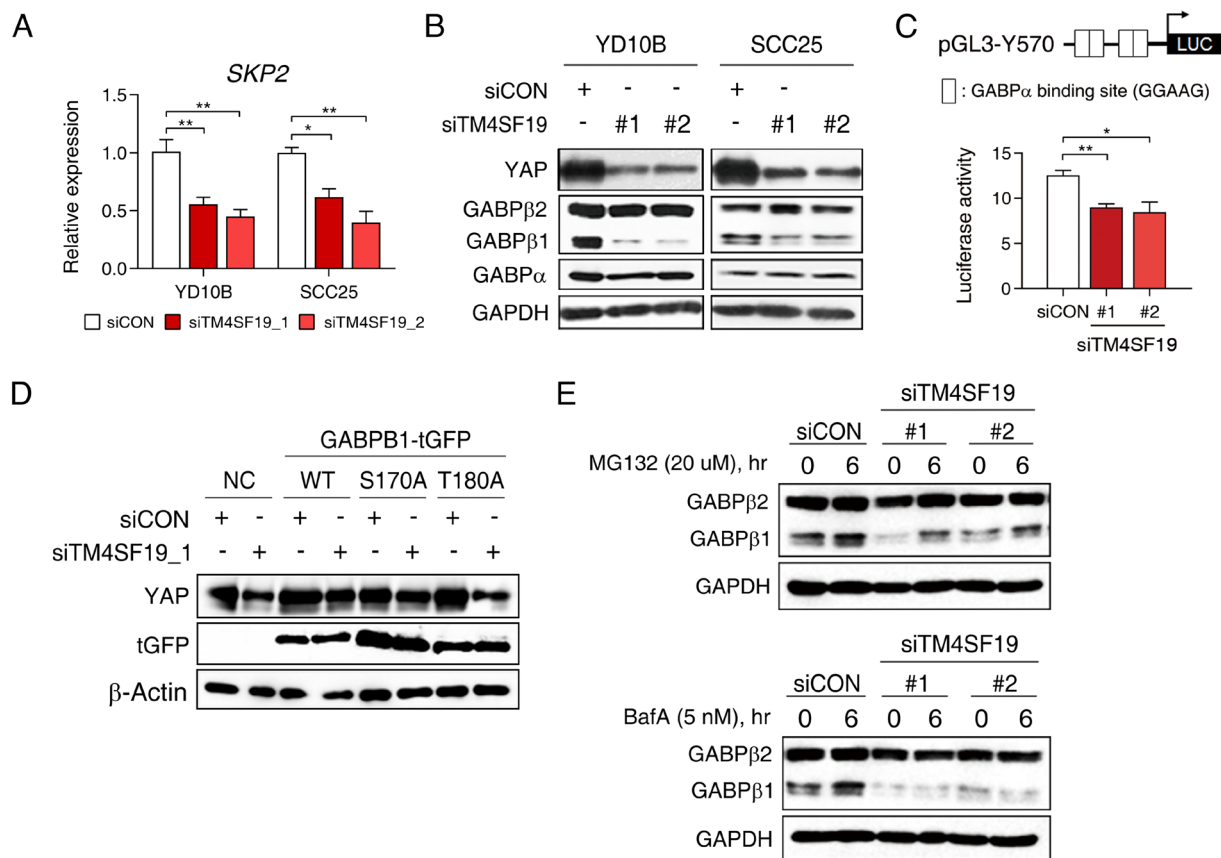


Fig. 3. Knockdown of TM4SF19 reduces YAP1 expression by down-regulating GABP β 1. (A) qRT-PCR analysis of SKP2 in YD10B cells after transfecting TM4SF19 siRNAs for 48 h compared to those with control siRNA. (B) Western blot of the indicated proteins in YD10B and SCC25 cells. Cells were transfected with siRNAs targeting TM4SF19 for 48 h. (C) Luciferase activity of pGL3-Y570 promoter in YD10B cells after cotransfection with siRNAs targeting TM4SF19 for 24 h. (D and E) Western blot of the indicated proteins in YD10B cells. (D) Cells were transfected with siRNAs targeting TM4SF19 for 48 h, followed by transfection of the indicated plasmids for 48 h. (E) Cells were transfected with siRNAs targeting TM4SF19 for 48 h, followed by MG132 or BafA treatments as stated. (A and C) Error bars indicate SEM ($n = 3$ independent experiments; * $P < 0.05$ and ** $P < 0.01$, unpaired t test).

Furthermore, when H_2O_2 -treated cells were washed, the up-regulated YAP levels decreased as the oxidized TM4SF19 gradually reduced (Fig. 4D). Pretreatment with the antioxidant N-acetyl cysteine (NAC) not only suppressed TM4SF19 oxidation but also prevented the increase in YAP in response to H_2O_2 treatment, suggesting that an oxidizing environment is necessary for up-regulating YAP expression (Fig. 4E). These results indicate that the homomeric cis-interaction of TM4SF19 is closely related to the oxidative stress-induced increase in YAP expression.

Next, we examined the subcellular localization of TM4SF19. While the L6 family members are commonly localized to the plasma membrane (38, 47), FLAG-tagged TM4SF19 was primarily detected in the cytoplasm near the nucleus, rather than in the plasma membrane (Fig. 4F and *SI Appendix*, Fig. S5A). FLAG-immunofluorescence colocalized with calnexin, a marker for the ER, whereas it did not colocalize with mitotracker, a marker for mitochondria (Fig. 4F and *SI Appendix*, Fig. S5 A and B). Although some L6 family members alter their subcellular localization for transmitting cellular signals (38, 48), the localization of TM4SF19 remained unchanged after H_2O_2 treatment (Fig. 4F and *SI Appendix*, Fig. S5 A and B).

Previous research demonstrated that the membrane topology of TM4SF20 is inverted by ceramide (49). To investigate whether TM4SF19 can be inverted in the ER membrane, we treated fixed cells with digitonin, which permeabilizes the plasma membrane, or NP-40, which permeabilizes both the plasma membrane and the ER membrane. Subsequently, we treated permeabilized cells

with proteinase K. As the FLAG epitope is tagged on the C terminus of TM4SF19, the FLAG-tag would be protected from proteinase K degradation if the C terminus is located in the ER lumen when cells are treated with digitonin. Results showed that when the ER membrane was intact, the monomer form of TM4SF19 was protected from degradation, while the dimer form was completely degraded (Fig. 4 G, Left). On the other hand, when the ER membrane was permeabilized by NP-40, both monomeric and dimeric TM4SF19 were degraded (Fig. 4 G, Right). These results indicate that topological localizations of TM4SF19 in the ER membrane differ between its monomeric and dimeric states, with the monomer favoring luminal localization of N and C termini, while the dimer favors cytosolic localization of N and C termini. To test whether oxidative stress can promote topology inversion of TM4SF19, we treated cells with either NAC or H_2O_2 and subsequently processed cells with digitonin and proteinase K. The immunofluorescence intensity of the FLAG-tag was significantly higher in H_2O_2 -treated cells compared to NAC-treated cells (Fig. 4H). Collectively, these findings suggest that TM4SF19 can exist as either monomers or dimers in the ER membrane, and oxidative stress promotes the equilibrium toward dimerization, which prefers the topology facing N and C termini to the cytosol (Fig. 4I).

Oxidative Stress Influences Physical Interactions between TM4SF19 and GABP β 1. We examined the potential physical interaction between TM4SF19 and GABP β 1. Immunoprecipitation

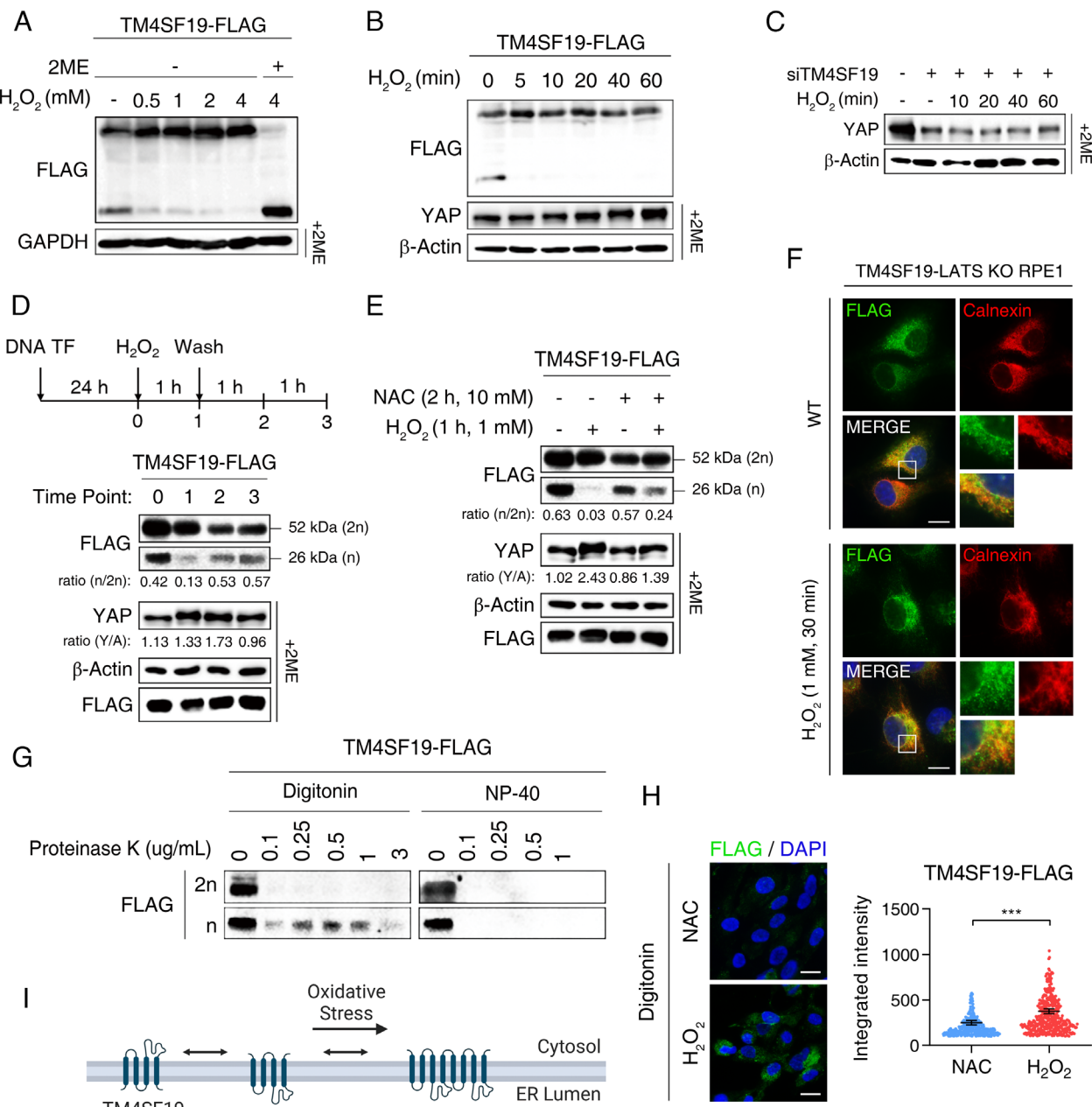


Fig. 4. Oxidative stress induces inversion and cis-interaction of TM4SF19 localized in the ER. (A–E) Western blot of the indicated proteins in YD10B cells. Nonreducing samples were prepared without 2-mercaptoethanol (2ME). (A and B) Cells were transfected with TM4SF19-FLAG plasmid for 24 h and treated with H_2O_2 varying concentrations for 10 min (A) or with 1 mM H_2O_2 for different periods of time (B). (C) Cells were transfected with siRNA targeting TM4SF19 for 48 h, followed by treatment of 1 mM H_2O_2 for the indicated time periods. (D) Cells were transfected with TM4SF19-FLAG plasmid for 24 h, followed by treatment with 1 mM H_2O_2 for 1 h and washing. Cells were then collected at different time points after washing. (E) Cells were transfected with TM4SF19-FLAG for 24 h, and then treated with H_2O_2 or NAC alone or in combination for a specific duration of time. The ratio of monomer to dimer TM4SF19 (n/2n) and YAP to β -Actin (Y/A) were calculated using ImageJ software. (F) Immunofluorescence staining of the indicated targets in YD10B cells after transfection of TM4SF19-FLAG plasmid for 24 h. (The scale bar represents 15 μ m.) (G) Western blot of FLAG in LATS1/2-null RPE1 cells with stable expression of TM4SF19 (TM4SF19-LATS KO RPE1). Cells were permeabilized by digitonin and then incubated with the indicated concentrations of proteinase K for 1 h with or without NP-40. (H) Immunofluorescence staining of the indicated protein in TM4SF19-LATS KO RPE1 cells (Left). Cells were incubated with either 10 mM NAC for 3 h or 1 mM H_2O_2 for 1 h before permeabilization using digitonin. Each dot in the graph represents the sum of pixel intensities within a cell (45). Error bars indicate SD ($n = 4$ independent experiments; *** $P < 0.001$, unpaired t test). (The scale bar represents 15 μ m.) (I) Expected model of TM4SF19 upon oxidative stress condition in HPV⁺ HNSCC. The illustration was created with BioRender (<https://biorender.com/>).

of FLAG-tagged TM4SF19 led to an increased amount of coprecipitated exogenously introduced and endogenous GABP β 1 (Fig. 5A and SI Appendix, Fig. S6A), indicating a potential physical interaction between TM4SF19 and GABP β 1. However, upon H_2O_2 treatment, the amount of coprecipitated GABP β 1 decreased (Fig. 5A and SI Appendix, Fig. S6A). This implies that oxidative stress-induced dimerization of TM4SF19 weakens its physical

interaction with GABP β 1 and that TM4SF19 dimers may protect GABP β 1 from degradation without direct physical interactions. Subcellular fractionation revealed that TM4SF19-FLAG localized to the cellular membrane, while GABP β 1 localized to both the cytosol and the nucleus (Fig. 5B and SI Appendix, Fig. S6B). The absence of the membrane-associated pool of GABP β 1 suggests that the physical interaction between TM4SF19 and GABP β 1 is

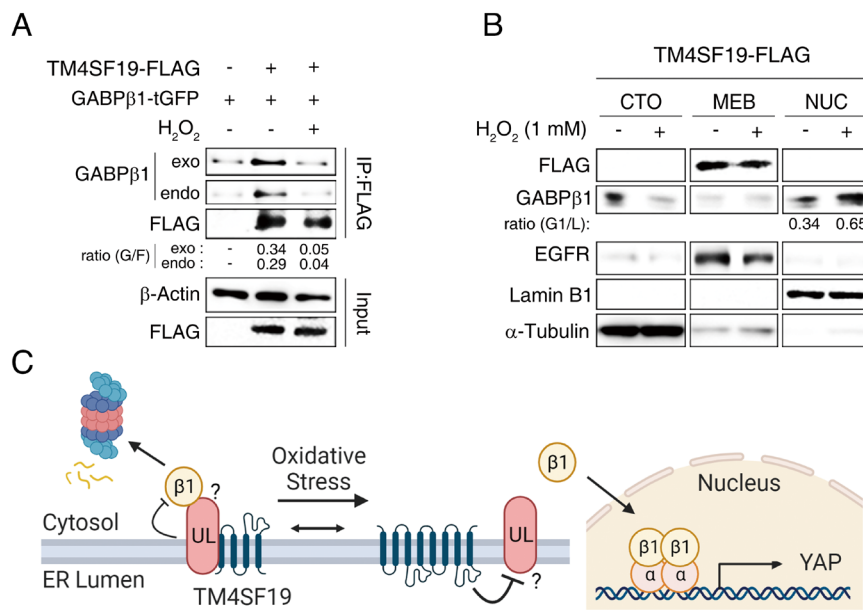


Fig. 5. Physical interaction between TM4SF19 and GABPβ1 is disrupted under oxidative stress conditions. (A) Coimmunoprecipitation analysis of TM4SF19 and GABPβ1. LATS1/2-null RPE1 cells were cotransfected with TM4SF19-FLAG and GABPβ1-tGFP for 24 h, and then treated with H₂O₂ for 1 h. The ratio of exogenous (exo) or endogenous (endo) GABPβ1 to FLAG-TM4SF19 (denoted as G/F) were calculated using ImageJ software. (B) Western blot of the indicated proteins in YD10B cells. Cells were transfected with TM4SF19-FLAG for 24 h, then subcellular protein fractionation was carried out following treatment with H₂O₂ for 1 h (CTO: cytosol, MEB: membrane compartment, NUC: nucleus). The ratio of GABPβ1 to Lamin B1 (denoted as G1/L) were calculated using ImageJ software. (C) Expected model of transcriptional regulation of YAP involving TM4SF19 in HPV- HNSCC. The illustration was created with BioRender (<https://biorender.com/>).

transient, and they do not form a stable complex. Importantly, the nuclear pool of GABPβ1 increased in response to H₂O₂ treatment (Fig. 5B and *SI Appendix*, Fig. S6B). Based on these results, we hypothesize that dimerized TM4SF19 may control the interaction between GABPβ1 and an unidentified regulator of GABPβ1 located in the ER membrane. Ubiquitin ligases associated with the ER could be potential candidates to mediate the link between TM4SF19 and GABPβ1 (Fig. 5C).

TM4SF19 Knockdown Suppresses Oncogenic Activity in Cancer Cells. We examined the impact of TM4SF19 knockdown on the oncogenic characteristics of OSCC cells. Immunofluorescence staining of Ki-67 was conducted, and a cell viability assay was performed after transfection with TM4SF19 siRNAs. TM4SF19 knockdown resulted in a significant reduction in both the proportion of Ki-67⁺ cells and overall cell viability (Fig. 6 A and B). In contrast, depletion of TM4SF19 in cells overexpressing the constitutively active form of YAP (YAP5SA) did not affect the number of Ki-67⁺ cells and its viability, confirming that YAP acts downstream of TM4SF19 (Fig. 6 C and D and *SI Appendix*, Fig. S7A). We next explored the impact of TM4SF19 depletion in UM-SCC47, a cell line derived from HPV⁺ HNSCC. TM4SF19 depletion efficiently decreased YAP1 transcription in UM-SCC47 cells (*SI Appendix*, Fig. S7B). However, intriguingly, neither TM4SF19 nor YAP depletion affected the survival of UM-SCC47 cells (*SI Appendix*, Fig. S7C). Notably, in UM-SCC47 cells, unlike in HPV- HNSCC cells, YAP was predominantly observed in the cytoplasm (*SI Appendix*, Fig. S7D). This observation suggests that HPV⁺ cells may undergo a YAP-independent cancerization process. We then performed an *in vitro* wound-healing assay, demonstrating that cells depleted of TM4SF19 exhibited slower closure of the scratched space compared to the control, indicating a decrease in cell migration due to TM4SF19 knockdown (*SI Appendix*, Fig. S7E and F). Moreover, gene ontology analysis of RNAseq data revealed downregulation of genes related to the cell cycle and DNA

replication upon TM4SF19 knockdown (*SI Appendix*, Fig. S7G). To explore the *in vivo* impact of TM4SF19 depletion, we utilized a xenograft mouse model using LATS1/2-null RPE1 cells, ensuring that YAP inhibition by the Hippo pathway was ruled out. Tumor growth was markedly accelerated in the group treated with DEM 3 d after xenograft, indicating a significant impact of oxidative stress on promoting cell proliferation during the early stages of tumor formation (Fig. 6E). Additionally, the tumor growth of cells expressing YAP5SA was significantly faster compared to that of the control group (Fig. 6F). We investigated the *in vivo* effect of TM4SF19 knockdown on tumor growth by introducing siRNAs into xenograft tumors via *in vivo* electroporation. As shown in Fig. 6G, TM4SF19 depletion effectively suppressed tumor growth. Moreover, *in vivo* electroporation of TM4SF19 siRNA led to a reduction in both mRNA and protein levels of YAP (Fig. 6 H and I). A combination of DEM and siRNA electroporation was not evaluated due to a synergistic cellular toxicity. These findings collectively suggest that TM4SF19 controls YAP1 expression and is essential for tumor cell proliferation, both *in vitro* and *in vivo*.

Discussion

ROS has the capability to modify the structure and function of crucial cellular macromolecules, including DNA. Oxidative DNA damage has been identified as a significant contributor to lung cancer, with smokers displaying a considerably higher mutational load compared to nonsmokers (50–52). Nevertheless, the relationship between oxidative stress and cancer is intricate and context-dependent. Evidence has been reported supporting both tumor-suppressive and oncogenic roles of NRF2 (53), adding complexity to the matter. Interestingly, in oral cancer, smoking does not lead to a statistically significant increase in the mutational load (7), suggesting that ROS generated by smoking and alcohol consumption may foster oral cancer progression through mechanisms other than DNA damage. In HNSCC, genes related to

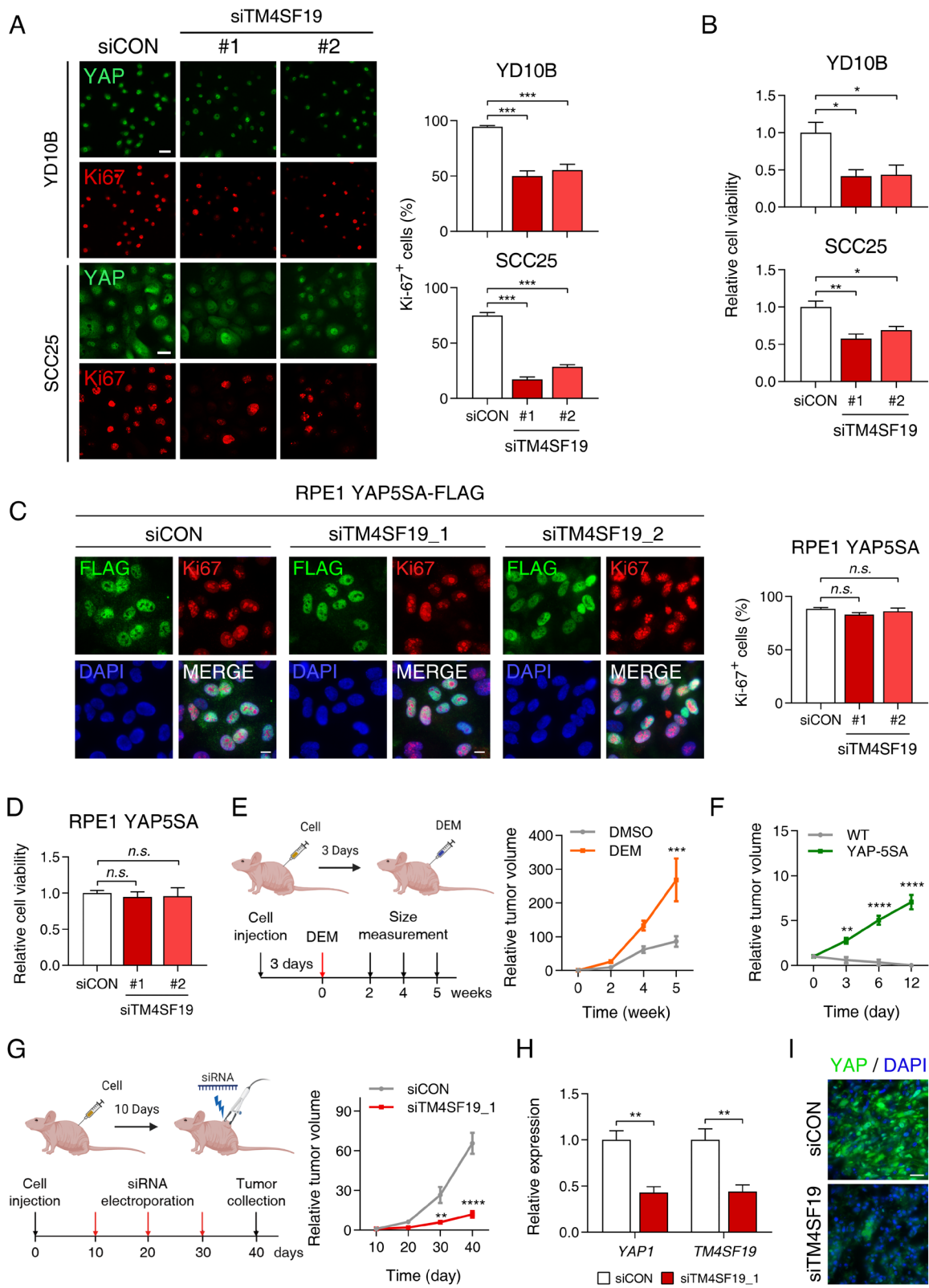


Fig. 6. Deletion of TM4SF19 suppresses the oncogenic activity of HPV[−] HNSCC. (A) Ki-67 staining images of YD10B and SCC25 cells transfected with either control or TM4SF19 siRNA for 72 h (Left, the scale bar represents 40 μ m), and percentage of Ki-67⁺ cells (Right). (B) Relative cell viability of YD10B and SCC25 cells after transfection with siRNAs targeting TM4SF19 for 72 h compared to those with control siRNA. (C) Ki-67 staining images of RPE1 YAP5SA-FLAG cells transfected with either control or TM4SF19 siRNA for 72 h (Left, the scale bar represents 15 μ m), and percentage of Ki-67⁺ cells (Right). (D) Relative cell viability of RPE1 YAP5SA-FLAG cells after transfection with siRNAs targeting TM4SF19 for 72 h compared to those with control siRNA. (E) Error bars indicate SEM ($n = 3$ independent experiments; * $P < 0.05$, ** $P < 0.01$, and *** $P < 0.001$, unpaired t test). (F) Relative volumes of LATS1/2-null RPE1 xenograft tumors after injecting DEM ($n = 3$ in each group). (G) Relative volumes of wild-type or YAP5SA-FLAG expressing RPE1 xenograft tumors ($n = 5$ in each group). (H) Error bars indicate SEM ($n = 4$ in each group; ** $P < 0.01$, unpaired t test). (I) Immunofluorescence staining of the indicated targets of xenograft tumor samples in Fig. 6G. (The scale bar represents 30 μ m.) (E and G) The illustrations were created with BioRender (<https://biorender.com/>).

oxidative stress are notably elevated, and their expression levels negatively correlate with patient survival rates (54). ROS can strongly affect various signaling pathways by creating intraprotein and interprotein bridges, thereby modifying their functions. Our study indicates that YAP upregulation through oxidative dimerization of TM4SF19 is a vital mechanism by which oxidative stress contributes to HPV[−] HNSCC development.

YAP is a known potent driver in the onset and progression of HPV[−] HNSCC. Supporting evidence includes a mouse model where hyperactivated YAP, through the removal of MOT1A/B, caused oral cancer to develop rapidly (within a month) (55). Conversely, inhibiting YAP suppressed oral cancer development (56). The Hippo pathway plays a central role in the posttranslational inhibition of the activity and stability of YAP. However, specific and potent Hippo pathway agonists are not yet available. Current therapeutic approaches targeting YAP focus on inhibiting protein–protein interactions with its binding partners. It is crucial to note, however, that *YAP1* transcription is elevated in various cancers, including HPV[−] HNSCC, compared to normal tissues (57–59). Elevated *YAP1* mRNA levels have been associated with a poor prognosis in specific cancers (60–62), further highlighting the importance of increased *YAP1* expression at the transcriptional level in promoting cancer development. Our findings suggest that transient yet repeated increases in *YAP1* gene transcription, triggered by oxidative stress due to smoking or alcohol consumption, may drive HPV[−] HNSCC development. Thus, inhibiting YAP at the transcriptional level presents an effective strategy for YAP inhibition.

The Hippo pathway appears to regulate *YAP1* gene transcription through GABP (25). Previous research has indicated that ROS-activated Hippo signaling suppresses GABP, which in turn leads to reduced *YAP1* expression under oxidative stress conditions. Contrary to this, our study has demonstrated that *YAP1* transcription increased when ROS levels were significantly raised in HPV[−] HNSCC cells. In this context, the amount of the GABP complex in the nucleus appears to have a greater influence on YAP expression than the total amount of GABP α . Furthermore, we found that oxidative stress–induced TM4SF19 activation promotes GABP β 1 stabilization. Because *TM4SF19* is expressed more highly in HPV[−] HNSCC than in liver cancer, its impact on GABP complex formation and GABP β 1 stability can be primarily observed in HPV[−] HNSCC. Our findings suggest that frequent gene amplification and increased expression of *TM4SF19* may play a critical role in HPV HNSCC development, thus redefining its significance from being considered merely a passenger event. While TM4SF19 appears to be a specific regulator of *YAP1* expression in cancer cells under oxidative stress, its expression in most normal adult cells remains low, making it unlikely that TM4SF19 is a general regulator of *YAP1* expression.

In our study, we demonstrated that TM4SF19 homodimerizes and rapidly up-regulates *YAP1* expression in response to oxidative stress, both *in vitro* and *in vivo*. However, the exact mechanism by which TM4SF19 regulates GABP complex formation and GABP β 1 stabilization remains elusive. Tetraspanins like TM4SF19 form structural platforms that recruit specific transmembrane proteins, forming tetraspanin-enriched microdomains, which could play a role in GABP regulation. Unlike other TM4SFs, that transmit extracellular signals at the plasma membrane, TM4SF19 is primarily located in the ER membrane. The sensitivity of TM4SF19 to ROS appears to be unique among TM4SFs, as others seem less suitable for sensing intracellular ROS, given that their loops forming disulfide bonds are exposed to the extracellular space. To further understand the mechanism behind YAP's transcriptional regulation, additional studies are required to identify the partner proteins of TM4SF19.

HPV[−] HNSCC that has spread and metastasized has a very poor prognosis. Although immune checkpoint inhibitor therapy shows promising results (63), a significant portion of patients does not respond favorably. EGFR and PIK3CA inhibitors are currently being used in HPV[−] HNSCC treatment (64), but YAP remains a promising target. Developing YAP-specific inhibitors with high efficiency continues to be a challenge. Our data suggest that inhibiting TM4SF19 not only decreases *YAP1* expression but also suppresses its transcriptional activity, offering an approach to inhibit hyperactivated YAP in cancers. The mechanisms involved in the link between YAP activation and TM4SF19-mediated YAP regulation is not clear. We speculate that intracellular oxidative stress conditions may influence the YAP-promoting function of TM4SF19. Inhibition of TM4SF19 may specifically suppress *YAP1* expression in cancer cells with high oxidative stress levels, while displaying low cytotoxicity in normal tissues. In conclusion, our study highlights the potential of TM4SF19 as a drug target to inhibit HPV[−] HNSCC and calls for further investigation into its function in HPV[−] HNSCC development.

Materials and Methods

For detailed materials and methods, see [SI Appendix](#).

Cell Culture. Human HPV[−] HNSCC cell line YD10B was obtained from the Korean Cell Line Bank, and SCC25 was obtained from American Type Culture Collection (ATCC) as frozen stocks to prevent contamination. Human HPV⁺ HNSCC cell line UM-SCC47 was kindly gifted by Dr. Yong Sun Lee (National Cancer Center, Korea). The cells were cultured in RPMI 1650 (Welgene) for YD10B, DMEM/F12 (Welgene) for RPE1 and SCC25 cells, and DMEM (Welgene) for UM-SCC47 cells supplemented with 10% FBS and 1% penicillin/streptomycin. All cell lines were used within 7 passages after reviving from the frozen stocks. Cells were treated with etoposide (50 μ M), hydrogen peroxide (H_2O_2) solution (1 mM), thapsigargin (5 μ M), tunicamycin (1 mM), or heat shock (45 °C) for 3 h to test the effect of HNSCC-associated external stresses on *YAP1* expression in Fig. 1B.

Protease Protection Assay. The protease protection assay was adapted from a previously published paper (49). For immunoblotting, cells were lysed with digitonin buffer [50 mM HEPES (pH 7.5), 150 mM NaCl, and 25 μ g/mL digitonin], supplemented with phosphatase inhibitors (Merck Millipore) on ice. Lysates, taken at 50 μ g per sample, were treated with varying amounts of proteinase K as indicated, either with or without 10% NP-40, and incubated for 1 h at 37 °C. The proteinase K degradation was halted by adding 5 mM of phenylmethylsulfonyl fluoride. For immunofluorescence, cells treated with NAC or H_2O_2 were fixed using 4% paraformaldehyde. Subsequently, they were exposed to 30 μ M digitonin for 10 min at room temperature. Following this, cells were incubated with the FLAG antibody for 1 h, and then 0.3 μ g/mL proteinase K was added for another 10 min. The reaction was then halted by treating with 1 mM of phenylmethylsulfonyl fluoride. The conjugated secondary antibodies were incubated as described in the immunofluorescence method section.

Datasets Analysis. TCGA data of different types of cancer were obtained from cBioPortal and normalized using RNA-Seq by Expectation-Maximization (RSEM) ([Dataset S1](#)). The gene expression data of normal and tumor samples of HNSCC patients were obtained from the Broad GDCA Firehose data portal and were normalized using RPKM ([Dataset S2](#)). Heatmapper online tool was used to generate the heatmap. In the correlation graphs, each dot represents the z-score values of gene expressions from individual patients. The RNA-seq dataset for the YD10B cell line was obtained from the Wellcome Sanger Institute.

Data, Materials, and Software Availability. All study data are included in the article and/or [supporting information](#).

ACKNOWLEDGMENTS. We would like to thank Dr. Yong Sun Lee (National Cancer Center, Korea) for providing UM-SCC47 HPV⁺ HNSCC cell line. We also thank the members of the J. Kim lab for critical discussions. This study was supported by the National Research Foundation of Korea grant funded by the Korean Ministry of Science (2020R1A2C3007748 and 2021R1A4A1032094).

1. Y. G. Eun *et al.*, Clinical significance of YAP1 activation in head and neck squamous cell carcinoma. *Oncotarget* **8**, 111130–111143 (2017).
2. S. Syrjänen, Human papillomavirus (HPV) in head and neck cancer. *J. Clin. Virol.* **32**, 59–66 (2005).
3. A. Argiris, M. V. Karamouzis, D. Raben, R. L. Ferris, Head and neck cancer. *Lancet* **371**, 1695–1709 (2008).
4. A. Argiris *et al.*, Evidence-based treatment options in recurrent and/or metastatic squamous cell carcinoma of the head and neck. *Front. Oncol.* **7**, 72 (2017).
5. K. K. Ang *et al.*, Human papillomavirus and survival of patients with oropharyngeal cancer. *N. Engl. J. Med.* **363**, 24–35 (2010).
6. D. E. Johnson *et al.*, Head and neck squamous cell carcinoma. *Nat. Rev. Dis. Primers* **6**, 92 (2020).
7. L. B. Alexandrov *et al.*, Mutational signatures associated with tobacco smoking in human cancer. *Science* **354**, 618–622 (2016).
8. B. Perillo *et al.*, ROS in cancer therapy: The bright side of the moon. *Exp. Mol. Med.* **52**, 192–203 (2020).
9. H. J. Forman, H. Zhang, Targeting oxidative stress in disease: Promise and limitations of antioxidant therapy. *Nat. Rev. Drug Discov.* **20**, 689–709 (2021).
10. D. Dequanter, R. Dok, S. Nuysts, Basal oxidative stress ratio of head and neck squamous cell carcinomas correlates with nodal metastatic spread in patients under therapy. *Onco. Targets Ther.* **10**, 259–263 (2017).
11. A. Stornetta, V. Guidolin, S. Balbo, Alcohol-derived acetaldehyde exposure in the oral cavity. *Cancers (Basel)* **10**, 20 (2018).
12. R. Visconti, D. Grieco, New insights on oxidative stress in cancer. *Curr. Opin. Drug. Discov. Devel.* **12**, 240–245 (2009).
13. M. Redza-Dutordoir, D. A. Averill-Bates, Activation of apoptosis signalling pathways by reactive oxygen species. *Biochim. Biophys. Acta* **1863**, 2977–2992 (2016).
14. Y. Wang *et al.*, Comprehensive molecular characterization of the hippo signaling pathway in cancer. *Cell Rep.* **25**, 1304–1317.e5 (2018).
15. F. Zanconato, M. Cordenonsi, S. Piccolo, YAP/TAZ at the roots of cancer. *Cancer Cell* **29**, 783–803 (2016).
16. R. Johnson, G. Halder, The two faces of Hippo: Targeting the Hippo pathway for regenerative medicine and cancer treatment. *Nat. Rev. Drug Discov.* **13**, 63–79 (2014).
17. F. X. Yu, B. Zhao, K. L. Guan, Hippo pathway in organ size control, tissue homeostasis, and cancer. *Cell* **163**, 811–828 (2015).
18. J. R. Misra, K. D. Irvine, The hippo signaling network and its biological functions. *Annu. Rev. Genet.* **52**, 65–87 (2018).
19. N. Chen *et al.*, YAP1 maintains active chromatin state in head and neck squamous cell carcinomas that promotes tumorigenesis through cooperation with BRD4. *Cell Rep.* **39**, 110970 (2022).
20. S. V. Saladi *et al.*, ACTL6A is co-amplified with p63 in squamous cell carcinoma to drive YAP activation, regressive proliferation, and poor prognosis. *Cancer Cell* **31**, 35–49 (2017).
21. S. A. Danovi *et al.*, Yes-associated protein (YAP) is a critical mediator of c-Jun-dependent apoptosis. *Cell Death Differ.* **15**, 217–219 (2008).
22. Y. Qiao, Y. Qian, J. Wang, X. Tang, Melanoma cell adhesion molecule stimulates yes-associated protein transcription by enhancing CREB activity via c-Jun/c-Fos in hepatocellular carcinoma cells. *Oncol. Lett.* **11**, 3702–3708 (2016).
23. W. M. Konsavage Jr., S. L. Kyler, S. A. Rennoll, G. Jin, G. S. Yochum, Wnt/beta-catenin signaling regulates Yes-associated protein (YAP) gene expression in colorectal carcinoma cells. *J. Biol. Chem.* **287**, 11730–11739 (2012).
24. A. M. Liu, R. T. Poon, J. M. Luk, MicroRNA-375 targets Hippo-signaling effector YAP in liver cancer and inhibits tumor properties. *Biochem. Biophys. Res. Commun.* **394**, 623–627 (2010).
25. H. Wu *et al.*, The Ets transcription factor GABP is a component of the hippo pathway essential for growth and antioxidant defense. *Cell Rep.* **3**, 1663–1677 (2013).
26. A. D. Sharrocks, The ETS-domain transcription factor family. *Nat. Rev. Mol. Cell Biol.* **2**, 827–837 (2001).
27. A. G. Rosmarin, K. K. Resendes, Z. Yang, J. N. McMillan, S. L. Fleming, GA-binding protein transcription factor: A review of GABP as an integrator of intracellular signaling and protein–protein interactions. *Blood Cells Mol. Dis.* **32**, 143–154 (2004).
28. R. J. Bell *et al.*, The transcription factor GABP selectively binds and activates the mutant TERT promoter in cancer. *Science* **348**, 1036–1039 (2015).
29. L. Ouyang, K. K. Jacob, F. M. Stanley, GABP mediates insulin-increased prolactin gene transcription. *J. Biol. Chem.* **271**, 10425–10428 (1996).
30. M. E. Martin, Y. Chinenov, M. Yu, T. K. Schmidt, X. Y. Yang, Redox regulation of GA-binding protein-alpha DNA binding activity. *J. Biol. Chem.* **271**, 25617–25623 (1996).
31. Y. Chinenov, T. Schmidt, X.-Y. Yang, M. E. Martin, Identification of redox-sensitive cysteines in GA-binding protein- α that regulate DNA binding and heterodimerization. *J. Biol. Chem.* **273**, 6203–6209 (1998).
32. J. W. Lee, Transmembrane 4 L six family member 5 (TM4SF5)-Mediated epithelial-mesenchymal transition in liver diseases. *Int. Rev. Cell Mol. Biol.* **319**, 141–163 (2015).
33. M. E. Hemler, Tetraspanin functions and associated microdomains. *Nat. Rev. Mol. Cell Biol.* **6**, 801–811 (2005).
34. Y. K. Huang, X. G. Fan, F. Qiu, TM4SF1 promotes proliferation, invasion, and metastasis in human liver cancer cells. *Int. J. Mol. Sci.* **17**, 661 (2016).
35. Y. W. Chang *et al.*, CD13 (aminopeptidase N) can associate with tumor-associated antigen L6 and enhance the motility of human lung cancer cells. *Int. J. Cancer* **116**, 243–252 (2005).
36. L. Ye *et al.*, Transmembrane 4 L-six family member-1 (TM4SF1) promotes non-small cell lung cancer proliferation, invasion and chemo-resistance through regulating the DDR1/Akt/ERK-mTOR axis. *Respir. Res.* **20**, 106 (2019).
37. S. C. Shih *et al.*, The L6 protein TM4SF1 is critical for endothelial cell function and tumor angiogenesis. *Cancer Res.* **69**, 3272–3277 (2009).
38. J. W. Jung *et al.*, Transmembrane 4 L six family member 5 senses arginine for mTORC1 signaling. *Cell Metab.* **29**, 1306–1319.e7 (2019).
39. C.-T. Chung *et al.*, Molecular profiling of afatinib-resistant non-small cell lung cancer cells in vivo derived from mice. *Pharmacol. Res.* **161**, 105183 (2020).
40. Z. B. Ke *et al.*, A radiation resistance related index for biochemical recurrence and tumor immune environment in prostate cancer patients. *Comput. Biol. Med.* **146**, 105711 (2022).
41. E. Shin, J. Kim, The potential role of YAP in head and neck squamous cell carcinoma. *Exp. Mol. Med.* **52**, 1264–1274 (2020).
42. L. Zender *et al.*, Identification and validation of oncogenes in liver cancer using an integrative genomic approach. *Cell* **125**, 1253–1267 (2006).
43. J. Seo *et al.*, MK5 regulates YAP stability and is a molecular target in YAP-driven cancers. *Cancer Res.* **79**, 6139–6152 (2019).
44. Y. J. Kim *et al.*, Genome-wide RNA interference screening reveals a COP1-MAP2K3 pathway required for YAP regulation. *Proc. Natl. Acad. Sci. U.S.A.* **117**, 19994–20003 (2020).
45. M. D. Wright, J. Ni, G. B. Rudy, The L6 membrane proteins—A new four-transmembrane superfamily. *Protein Sci.* **9**, 1594–1600 (2000).
46. S. van Deventer, A. B. Arp, A. B. van Spriel, Dynamic plasma membrane organization: A complex symphony. *Trends Cell Biol.* **31**, 119–129 (2021).
47. C.-I. Lin *et al.*, TM4SF1: A new vascular therapeutic target in cancer. *Angiogenesis* **17**, 897–907 (2014).
48. T. E. Sciuто *et al.*, Intracellular distribution of TM4SF1 and internalization of TM4SF1 antibody complex in vascular endothelial cells. *Biochem. Biophys. Res. Commun.* **465**, 338–343 (2015).
49. Q. Chen *et al.*, Inverting the topology of a transmembrane protein by regulating the translocation of the first transmembrane helix. *Mol. Cell* **63**, 567–578 (2016).
50. C. Cao *et al.*, Smoking-promoted oxidative DNA damage response is highly correlated to lung carcinogenesis. *Oncotarget* **7**, 18919–18926 (2016).
51. Z. Chen *et al.*, Oxidative DNA damage is involved in cigarette smoke-induced lung injury in rats. *Environ. Health Preventive Med.* **20**, 318–324 (2015).
52. T. Paz-Elizur *et al.*, DNA repair activity for oxidative damage and risk of lung cancer. *J. Natl. Cancer Inst.* **95**, 1312–1319 (2003).
53. M. Rojo de la Vega, E. Chapman, D. D. Zhang, NRF2 and the Hallmarks of Cancer. *Cancer Cell* **34**, 21–43 (2018).
54. A. Leone, M. S. Roca, C. Ciardiello, S. Costantini, A. Budillon, Oxidative stress gene expression profile correlates with cancer patient poor prognosis: Identification of crucial pathways might select novel therapeutic approaches. *Oxid. Med. Cell Longev.* **2017**, 2597581 (2017).
55. H. Omori *et al.*, YAP1 is a potent driver of the onset and progression of oral squamous cell carcinoma. *Sci. Adv.* **6**, eay3324 (2020).
56. S. E. Hiemer *et al.*, A YAP/TAZ-regulated molecular signature is associated with oral squamous cell carcinoma. *Mol. Cancer Res.* **13**, 957–968 (2015).
57. J.-J. Cao *et al.*, YAP is overexpressed in clear cell renal cell carcinoma and its knockdown reduces cell proliferation and induces cell cycle arrest and apoptosis. *Oncol. Rep.* **32**, 1594–1600 (2014).
58. M. Z. Xu *et al.*, Yes-associated protein is an independent prognostic marker in hepatocellular carcinoma. *Cancer* **115**, 4576–4585 (2009).
59. D. Zhou *et al.*, Mst1 and Mst2 protein kinases restrain intestinal stem cell proliferation and colonic tumorigenesis by inhibition of Yes-associated protein (Yap) overabundance. *Proc. Natl. Acad. Sci. U.S.A.* **108**, E1312–E1320 (2011).
60. L. Guo, Y. Chen, J. Luo, J. Zheng, G. Shao, YAP1 overexpression is associated with poor prognosis of breast cancer patients and induces breast cancer cell growth by inhibiting PTEN. *FEBS Open Bio.* **9**, 437–445 (2019).
61. G.-X. Zhou *et al.*, Effects of the hippo signaling pathway in human gastric cancer. *Asian Pac. J. Cancer Prev.* **14**, 5199–5205 (2013).
62. X. Hu *et al.*, The role of YAP1 in survival prediction, immune modulation, and drug response: A pan-cancer perspective. *Front. Immunol.* **13**, 1012173 (2022).
63. Z. Mei, J. Huang, B. Qiao, A.K.-Y. Lam, Immune checkpoint pathways in immunotherapy for head and neck squamous cell carcinoma. *Int. J. Oral Sci.* **12**, 16 (2020).
64. Q. Li, Y. Tie, A. Alu, X. Ma, H. Shi, Targeted therapy for head and neck cancer: Signaling pathways and clinical studies. *Signal Transduct. Target. Ther.* **8**, 31 (2023).